

© 2023 Author(s). Published under an exclusive license by AIP Publishing.
<https://doi.org/10.1063/5.0143619>

Cite:

Isaac Carrillo-Acuña, Juan Edson Villanueva-Tiburcio, Braulio Gutiérrez-Medina; An efficient optical diffuser fabricated from fungal mycelium. *Appl. Phys. Lett.* 13 March 2023; 122 (11): 113702.
<https://doi.org/10.1063/5.0143619>

RESEARCH ARTICLE | MARCH 14 2023

An efficient optical diffuser fabricated from fungal mycelium




Isaac Carrillo-Acuña ; Juan Edson Villanueva-Tiburcio ; Braulio Gutiérrez-Medina

Check for updates

Appl. Phys. Lett. 122, 113702 (2023)

<https://doi.org/10.1063/5.0143619>





Instruments for Advanced Science


- Knowledge
- Experience
- Expertise

Click to view our product catalogue

Contact Hiden Analytical for further details:

www.HidenAnalytical.com
info@hiden.co.uk

Gas Analysis




- ▶ dynamic measurement of reaction gas streams
- ▶ catalysis and thermal analysis
- ▶ molecular beam studies
- ▶ dissolved species probes
- ▶ fermentation, environmental and ecological studies

Surface Science



- ▶ UHV TPD
- ▶ SIMS
- ▶ end point detection in ion beam etch
- ▶ elemental imaging - surface mapping

Plasma Diagnostics



- ▶ plasma source characterization
- ▶ etch and deposition process reaction kinetic studies
- ▶ analysis of neutral and radical species

Vacuum Analysis



- ▶ partial pressure measurement and control of process gases
- ▶ reactive sputter process control
- ▶ vacuum diagnostics
- ▶ vacuum coating process monitoring

An efficient optical diffuser fabricated from fungal mycelium

Cite as: Appl. Phys. Lett. **122**, 113702 (2023); doi: [10.1063/5.0143619](https://doi.org/10.1063/5.0143619)

Submitted: 24 January 2023 · Accepted: 3 March 2023 ·

Published Online: 14 March 2023



View Online



Export Citation



CrossMark

Isaac Carrillo-Acuña,¹  Juan Edson Villanueva-Tiburcio,²  and Braulio Cutiérrez-Medina^{1,a)} 

AFFILIATIONS

¹Division of Advanced Materials, Instituto Potosino de Investigación Científica y Tecnológica, Camino a la Presa San José 2055, San Luis Potosí 78216, Mexico

²Escuela Profesional de Ingeniería Agroindustrial, Universidad Nacional Hermilio Valdizán, Av. Esteban Pabletich 172, Pillco Marca, Huánuco, Peru

^{a)}Author to whom correspondence should be addressed: bgutierrez@ipicyt.edu.mx. Tel.: 52 (444) 834-2000

ABSTRACT

Scattering of light from randomly textured materials is ubiquitous and of great interest in biology and for diverse applications—including filtering, light trapping in solar cells, and speckle photography. One attractive means to build these materials is by harnessing the complexity present in structures of biological origin. Here, we report on the development of a random phase diffuser based on intertwined filamentous cells (hyphae) of the fungus *Trichoderma atroviride*. A fungal colony (mycelium) is grown on the surface of a gel medium, and then removed, fixated, and dehydrated, resulting in a free-standing, two-dimensional random mesh ($1\text{ cm} \times 1\text{ cm} \times 5\text{ }\mu\text{m}$) composed of rigid hyphae separated by air gaps. A laser beam incident on the bioplate results in speckle patterns of nearly equal intensity in transmission and reflection. By modeling the bioplate as composed of optical phase elements and computing Fraunhofer diffraction, we recover the overall shape of the observed diffuse light spot. As the hyphal density composing the sample is increased, all optical power is in the speckle pattern, and approximate Lambertian transmissivity is reached. Altogether, our observations suggest that a planar fungal colony can scatter light efficiently by imparting a random phase. These results underscore the potential of a biological structure to develop optical elements and to use light scattering to evaluate morphology in complex structures—such as filamentous mycelia.

Published under an exclusive license by AIP Publishing. <https://doi.org/10.1063/5.0143619>

Scattering of light by randomly textured materials is ubiquitously present in everyday experience (even in mirrors), and light patterns resulting from this phenomenon contain essential information regarding the composition and morphology of materials from which light is reflected or transmitted. Accordingly, the study of randomness in optically diffusing surfaces or diffractive elements is of great interest in applications that include layers of random morphology to enhance optical absorption in solar cells (light trapping),^{1–3} sensors developed in speckle photography,^{4–6} and optical filters based on diffraction gratings.^{7,8} From the optical point of view, the distinctive feature of randomly textured materials is their ability to distribute light over all scattering angles, and their associated speckle patterns can reflect negligible changes in the structure of the random texture.

One attractive strategy to develop random structures of optical interest is the use of biological scaffolds. Biological systems offer abundant architectures with diverse morphologies that can be exploited in materials synthesis and functionalization. To date, a wide variety of biological building blocks, such as DNA,⁹ proteins,¹⁰ viruses,¹¹

bacteria,¹² algae, insects,¹³ and fungi,¹⁴ have been used as biotemplates with diverse physical properties. The micro- and nanostructures found in biosystems offer rapid generation times, simple processes for growth and preparation,¹⁵ and present both ordered,¹⁶ and irregular patterns.¹⁷ The applications of schemes that mimic biological structures are wide, ranging from electronics¹⁸ to manipulation in solar energy.¹⁹ While optical scattering produced by periodical arrays is a well-studied process, there is considerably less research regarding random diffraction produced by biological structures. Notably, it has been found that certain types of coloration present in the wings of insects and the feathers of birds are due to light scattering from non-periodic and random structures.^{20–22} Furthermore, there is significant biotechnological interest in using light scattering to develop analytical tools that characterize the highly complex morphology of filamentous fungus of the type described below.²³

In this study, we present fabrication and optical characterization of an optical diffuser based on a biotemplate. To provide random texture, we chose the filamentous fungus *Trichoderma atroviride*, an

organism of interest in biotechnology and agriculture.²⁴ In filamentous fungi, cells are arranged as filaments (known as hyphae), and vegetative growth consists of hyphae elongating at the apices and undergoing branching. The colony that develops is the mycelium—a collective of highly intertwined filamentous hyphae. We show that planar mycelia can act as optical diffractive plates of the phase kind, and control of the hyphal density results in efficient transfer of optical power to the scattered light.

We grow two-dimensional *T. atroviride* colonies in Petri dishes [Fig. 1(a)] by inoculating conidia ($\sim 10\text{-}\mu\text{m}$ diameter spores) at the center of 8-cm diameter cellophane disks placed directly over the potato dextrose agar (PDA) solid medium. Inoculation of *T. atroviride* on cellophane paper allowed us to separate the fungal film without compromising its structure. Colonies were developed at 28°C under dark conditions; the absence of light ensured vegetative growth (avoiding the development of asexual reproduction structures),²⁵ thus maintaining a mycelium composed exclusively of intertwined hyphae. Under these conditions, the mycelium exhibits radial growth in the plate [Fig. 1(b)].

The fabrication process is shown in Fig. 1(c). All chemicals were purchased from Sigma Aldrich, except where indicated. Fungal cultures were grown for 36 h, well before the colony filled the plate

[see Fig. 1(b)], therefore ensuring a healthy and reproducible structure. In an aseptic environment, $\sim 100\text{ mm}^2$ areas of cellophane with young mycelium were trimmed (from the edge of the colony) for further treatment. The mycelium cuttings were fixed in 4% paraformaldehyde (PFA) diluted in phosphate-buffered saline (PBS) for 4 h. Samples were washed by rinsing three times with PBS for 15 min each and then dehydrated in graded ethanol (35%, 50%, 75%, and 95% ETOH) and two exchanges of anhydrous 100% ETOH) followed by two exchanges in anhydrous acetone. Finally, samples were left to dry onto microscope slides. This preparation produced free-standing pellicles, although most of the observations reported here were performed by sandwiching samples between a glass slide and a coverslip. The sandwich condition protects the otherwise fragile samples, extending the useful life of the bioplate to several months.

Figure 2(a) presents the resulting bioplate. Observation under the bright-field (BF) optical microscope [Fig. 2(b)] reveals an intricate mesh formed by filaments and interspaces of irregular size and shapes. The arrangement of hyphae has a broad distribution of spatial frequencies with no discernable periodic components [Fig. 2(c)] and wide histograms of inter-hyphal space area [Figs. 2(d)–2(f)]. Samples show a spatial gradient in the density of hyphae (in the mm range): low, middle, and high, at 0, ~ 3 , and $\sim 6\text{--}10$ mm into the colony from the edge, respectively [Figs. 2(d)–2(f)]. Moreover, from scanning electron microscopy (SEM) micrographs (obtained by mounting $\sim 5\text{ mm}^2$ free-standing bioplates on carbon tape; FEI Quanta 250, 80 Pa, 8–12 kV), hyphae are seen to be embedded in the PFA matrix and leaving the irregular inter-hyphae spaces empty [Fig. 2(g)].

From the SEM images, we assess that the thickness of our samples is $\sim 5\text{ }\mu\text{m}$ [Fig. 2(h)]. We performed another, independent measurement of the sample thickness by using the glass slide and coverslip enclosing a bioplate as an etalon. As this configuration was illuminated with a laser beam ($\lambda = 450\text{ nm}$), light reflecting from the inner (uncoated) glass surfaces of the enclosure underwent interference at a projection screen located a distance l from the etalon, thus producing well-known concentric circular fringes. In the small angle approximation, the distance between the glass surfaces (and, therefore, the thickness of the bioplate) is $s = \lambda l^2 / (y_m^2 - y_{m+1}^2)$, where y_m is the radius of the m th fringe. By measuring the radii of these fringes, the thickness was measured, $s = 5.9 \pm 0.6\text{ }\mu\text{m}$. Altogether, these results show that the bioplates are two dimensional (with typical dimensions $5\text{ mm} \times 5\text{ mm} \times 6\text{ }\mu\text{m}$), the structure is formed essentially by two types of elements: hyphae and inter-hyphae empty spaces, and the distribution of these elements is random.

To evaluate the optical properties of our bioplate, we first measured the transmittance (T) and reflectance (R) properties of the sample with a high density of hyphae [Fig. 3(a)]. The R–T curve was measured using an integrating sphere (Newport, 819C-SF-4) with Spectralect as the inner-sphere material (96%–98% reflectivity from 400 to 800 nm). Diffuse light measurements were performed with a spectrometer coupled to the integrating sphere, showing samples with $\sim 60\%$ and 40% transmittance and reflectance, respectively, in the 450–900 nm spectral range with little optical absorbance. Next, we built an optical setup to characterize the patterns of diffuse light produced by the bioplates under coherent illumination [Fig. 3(b)]. A He–Ne laser beam ($\lambda = 632.8\text{ nm}$, Thorlabs HNL150RB) with a Gaussian profile ($800\text{ }\mu\text{m}$ in width) incident on the plates results in a speckle pattern both in transmission and reflection with a wide angular

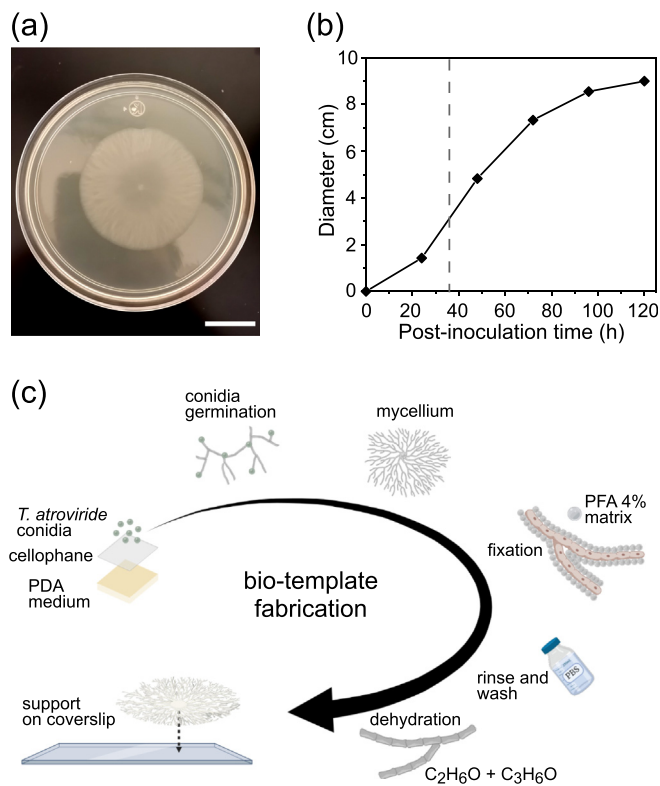


FIG. 1. Biological sample and its preparation. (a) Colony of *T. atroviride* grown on cellophane in PDA plates for 36 h at 28°C in dark conditions (scale bar, 20 mm). (b) Fungal colony diameter over time. The vertical dashed line indicates the typical time when samples were taken for subsequent preparation. (c) Schematic representation for the fabrication procedure of the bioplate based on the fungus *T. atroviride*.

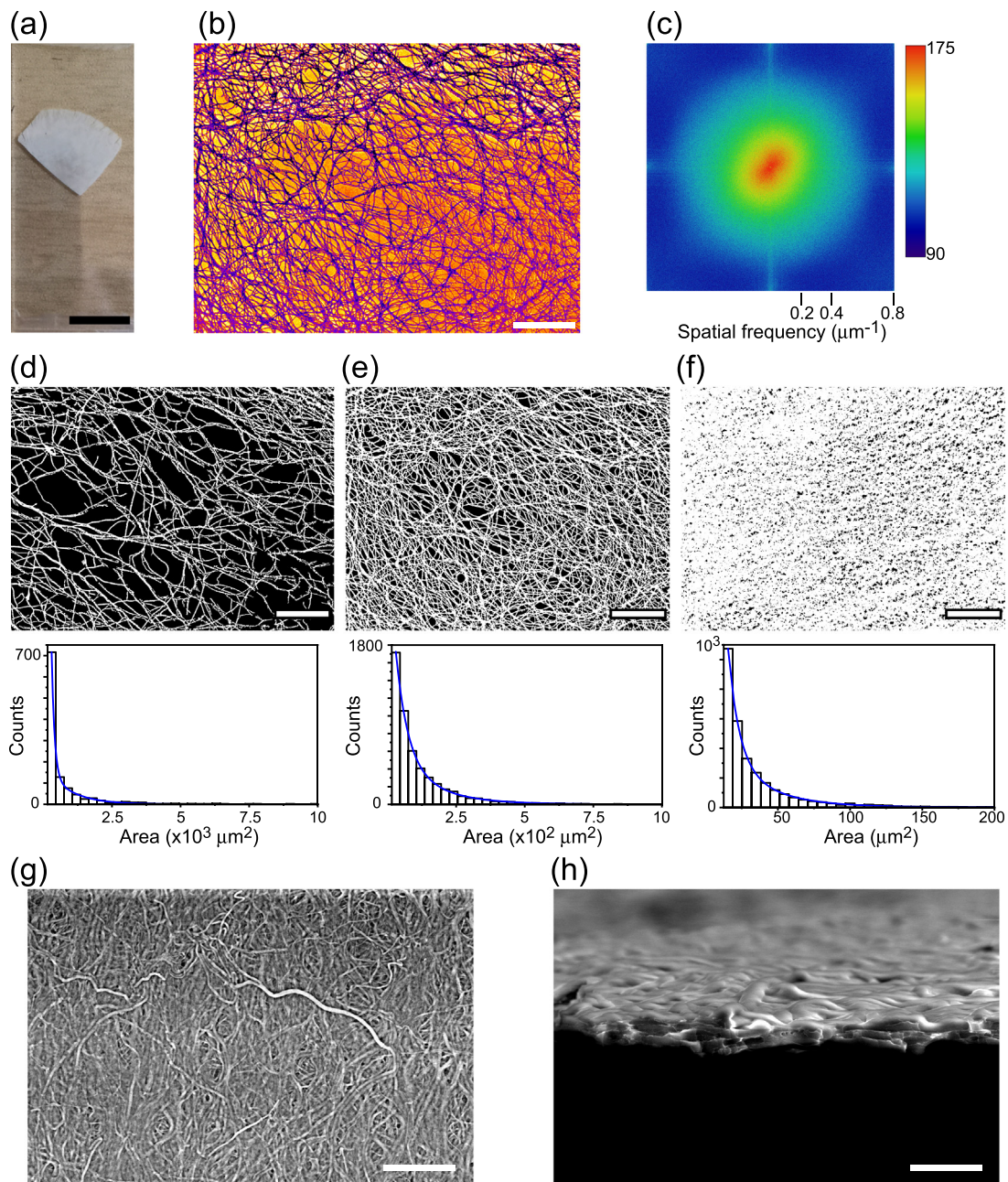


FIG. 2. Morphology of the bioplate fabricated from fungal mycelium. (a) Macroscopic view of the bioplate on a microscope slide (scale bar, 10 mm). (b) Bright-field (BF) microscopy shows the superficial texture of the bioplate (scale bar, 200 μm). (c) Fourier-transform of the image in (b). (d)–(f) Binarized, BF micrographs show low (d), medium (e), and high (f) hyphal densities; white color corresponds to fungal hyphae. Scale bar, 200 μm . The bottom row shows the corresponding histograms of the inter-hyphal space area, together with an exponential fit (blue lines); mean values of the inter-hyphal space area from the fit: $894 \pm 32 \mu\text{m}^2$ (low), $145 \pm 8 \mu\text{m}^2$ (medium), and $30 \pm 2 \mu\text{m}^2$ (high). (g)–(h) SEM micrographs of the bioplate. Scale bar, 100 μm (g) and 10 μm (h).

distribution. In transmission, at increased hyphal densities, the central undeflected laser spot vanishes [Fig. 3(b)], indicative of high scattering efficiency.

The intensity pattern produced by the diffuser is not circular [Figs. 4(a) and 4(b)], indicating that light is not undergoing multiple

scattering at the plate. Furthermore, as little absorption is observed [Fig. 3(a)], we conclude that the plate mainly acts by imparting phase to incoming light. To test this hypothesis, we consider the plate as a spatial arrangement of phase-imparting elements (the hyphae) and compute the expected Fraunhofer diffraction pattern resulting from a

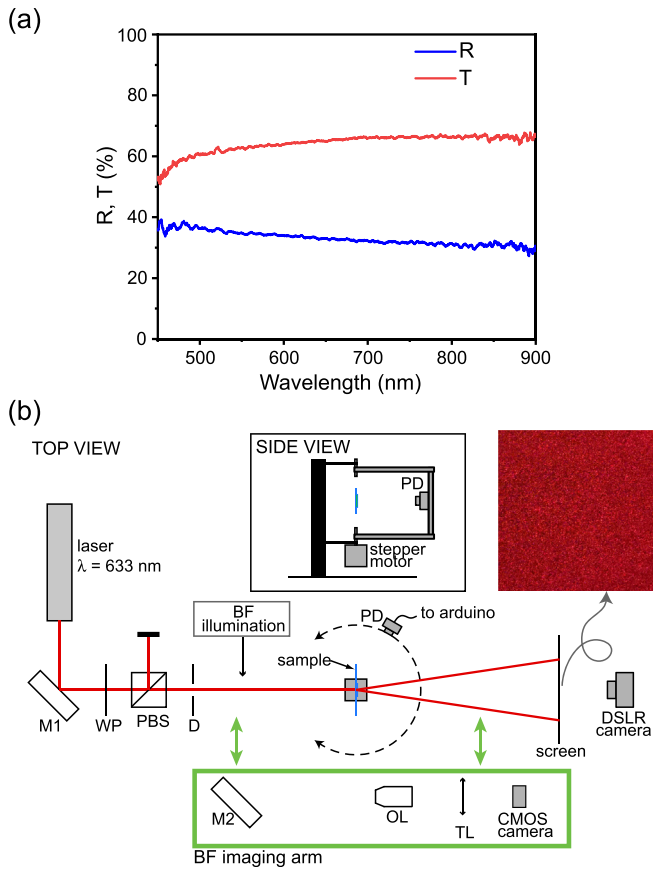


FIG. 3. (a) Reflectance (R) and transmittance (T) spectrum of the bioplate. (b) Schematic of the optical setup built to characterize the plate. A laser beam (red) impinges on the sample (blue), resulting in a wide-angled diffraction pattern that hits a translucent screen (upper right image), which is imaged by a digital camera (DSRL). The hyphal morphology responsible for the observed speckle pattern is imaged by inserting a bright field (BF) arm (green square) into the main optical axis; BF is adjusted for Kohler alignment. The side view shows the details of the photodiode (PD) mount to measure the angular distribution of the light intensity. M: mirror; WP: waveplate; PBS: polarization beam splitter cube; D: iris diaphragm; OL: objective lens; TL: tube lens.

monochromatic plane wave (wavelength λ) incident on the arranged phase elements. The hyphal arrangement is obtained from a bright-field microscopy digital image of the bioplate and, to compare against experimental results, the experimental diffusive pattern is recorded using a laser beam passing through the same imaged region. To use the digital image to compute diffracted light, we regard the bioplate as a holographic diffuser,²⁶ where the phase information is obtained from the image (see below).

Using the above considerations, we consider a plane wave incident on a collection of identical square apertures (corresponding to the pixels in the image) each acting as a phase element. The square aperture located at coordinate (l, m) will impart a phase $\Phi(l, m)$ onto the transmitted wave. The scattered field strength²⁷ results from the sum over all $(2M + 1) \times (2N + 1)$ square pixels in the digital image,

$$U(x, y, z) = \frac{e^{ikz} e^{ik(x^2+y^2)/2z}}{i\lambda z} \mathcal{F} \left\{ \sum_{m=-M}^M \sum_{l=-L}^L \text{rect} \left(\frac{\xi - 2lw}{2w} \right) \times \text{rect} \left(\frac{\eta - 2mw}{2w} \right) e^{i\Phi(l,m)} \right\} \Bigg|_{f_x = \frac{x}{\lambda z}, f_y = \frac{y}{\lambda z}} \quad (1)$$

where w is the half-width of pixels in the digital image, ξ and η are the orthogonal directions in the sample plane, $k = 2\pi/\lambda$, $i = \sqrt{-1}$, and \mathcal{F} is the Fourier transform operation. The phase imparted by each square aperture of the bioplate is modeled simply as $\Phi(l, m) = ksn_{l,m}$, where s is the thickness of the bioplate and $n_{l,m}$ is the refractive index of the square element with coordinate (l, m) . Evaluation of the transform in Eq. (1) yields

$$U(x, y, z) = U_0 \text{sinc} \left(\frac{2xw_x}{\lambda z} \right) \text{sinc} \left(\frac{2yw_y}{\lambda z} \right) \times \sum_{m=-M}^M \sum_{l=-L}^L e^{ik[sn_{l,m} - 2(xw_x l + yw_y m)/z]} \quad (2)$$

To obtain the refractive index map ($n_{l,m}$) from a digital image of the bioplate, we perform the following image processing operations. First, we remove the background and normalize the gray-level histogram of the image; then, an $n_{l,m}$ value is assigned to each pixel (l, m) using a linear relationship between n and the image gray level such that $n = 1.52$ for max(gray values) and $n = 1.0$ for min(gray values). In this approximation, we assume that the gray-level intensity of the image scales linearly with the refractive index. The maximum value $n = 1.52$ is used here as it has been found for fixed filamentous fungal samples.²⁸ The final light intensity distribution $I(x, y)$ to be compared with the experimental results from $I(x, y) = |U(x, y, z)|^2$, using Eq. (2) with $z = 1$ m.

A comparison of the observed diffusive light pattern with the result of the model reveals that the two patterns show qualitative agreement in the overall shape [Figs. 4(b) and 4(c)]. The disposition of hyphae in the sample [Fig. 4(a)] shows the random orientation superposed to a preferred direction—presumably related to the radial net direction of growth at the colony level; this cellular organization results in an elongated diffraction pattern whose main axis is rotated $\pi/2$ with respect to the preferred hyphal orientation. In both experiment and model, a dense and extended speckle pattern is observed, indicating a wide, random distribution of spatial frequencies in the sample. Provided that transmission diffusers produce light patterns whose characteristics depend on a number of factors (such as shadowing, refraction, and multiple scattering), and the bioplate is not exactly planar, the agreement of experiment with the results of our oversimplified model is remarkable and support the notion that the bioplate acts as an effective random diffuser of the phase kind.

We next aimed to evaluate the scattered light distribution produced by the fabricated bioplate. Using the home-made setup shown in Fig. 3(b), we measured the intensity of diffracted light as a function of the scattering angle for normal laser incidence (Fig. 5). A He-Ne laser beam ($\lambda = 633$ nm) was used for illumination, and the light intensity was recorded using a Si photodiode (Thorlabs DET110, 3.6² mm² active area) armed with an interference filter (633 ± 20 nm). To perform angular measurements, the photodiode is located at a distance of 115 mm from the bioplate and mounted on a stepped motor (NEMA-17, with its rotation axis centered at the intersection of the

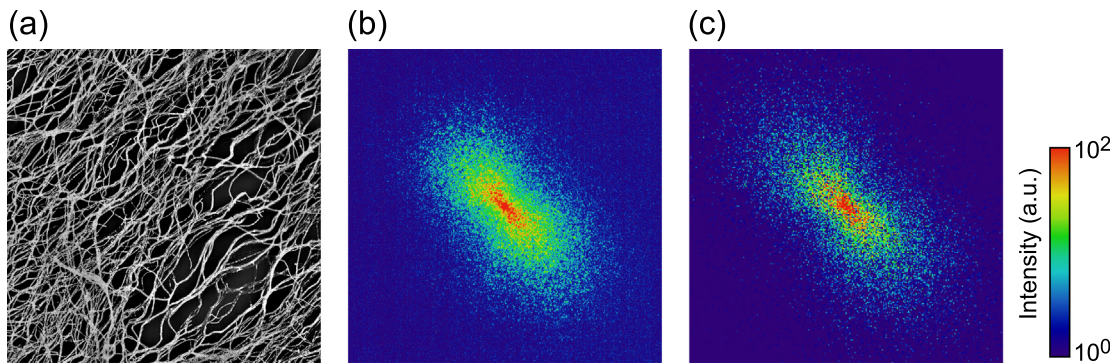


FIG. 4. Comparison of the computed and observed diffraction pattern produced by the bioplate. (a) BF image of the hyphal distribution composing the biological template. Field of view, $840 \times 840 \mu\text{m}^2$. (b) Experimental diffusive pattern produced by a laser beam impinging on the bioplate area shown in (a). (c) Diffraction pattern computed from the bioplate area shown in (a). Images shown after background removal. Field of view in (b) and (c), $10 \times 10 \text{ cm}^2$.

sample plane and the laser illumination beam, controlled via computer using an Arduino interface). A broad angular distribution is observed (Fig. 5) with width increasing as the hyphal density increases, in accordance with the expected behavior of a diffraction plate. In the densest probed sample [Fig. 5(c)], the undeflected beam vanishes, and nearly all optical power is distributed within the scattering pattern. This behavior signals a high-efficiency diffusive plate and suggests that Lambertian transmittivity can be achieved at the saturating hyphal density. Interestingly, as our measurements reach wide diffraction angles [see Fig. 5(c)], we notice significant diffractive power in reflection. This behavior, together with the nearly 50%–50% R–T curve displayed in Fig. 3(a), indicates that our bioplate is an excellent diffractive element able to distribute light power into nearly all angles.

Altogether, we have developed a randomly textured material with diffusive properties provided by a natural substrate. Our bioplate demonstrates simple, replicable, and cost-effective fabrication of a random phase diffractive element that can be morphologically modulated by adjusting fungal growth times. This approach contrasts with specialized procedures typically used in the construction of periodic and geometric micropatterns. One recently developed method to achieve ultrathin (subwavelength-thick) diffusers uses electron-beam lithography and reactive-ion etching to sculpt dielectric metasurfaces.²⁹ In our case, straightforward fabrication achieves thin ($<10 \mu\text{m}$ in thickness)

plates with efficient and nearly Lambertian optical diffusive behavior at a minimal cost (<1 USD per sample). The bioplate presented here could have potential application in flat photonic devices. In light trapping, for example, mold transfer and roll-to-roll processing³⁰ could produce copies of our random diffraction diffuser to be incorporated in solar cells. Apart from potential applications in light management, our results on the optical properties shown by mycelia grown on surfaces bear biotechnological interest. Indeed, we have shown that the hyphal density determines the efficiency and spread of the diffusive pattern. This characteristic could be used to record scattered light patterns and evaluate from them the complex fungal morphology³¹ without resorting to optical microscopy and image processing methods.³² Previous experiments have shown a linear correlation between the intensity of backscattered light and the mycelium dry weight.²³ We speculate that analysis of the diffusive light patterns of the kind reported in the present work could be used to evaluate *in-vivo* hyphal density or other mycelial complexity metrics such as fractal dimension.³³ We will explore this possibility in future studies.

Finally, our work parallels previous efforts that use microorganisms as bio-templates, such as studies that use bacteria to direct the construction of hollow TiO_2 structures applied for light harvesting through scattering.³⁴ Supported by substrates, these bioplates constitute excellent molds to be reproduced. Future improvements to our

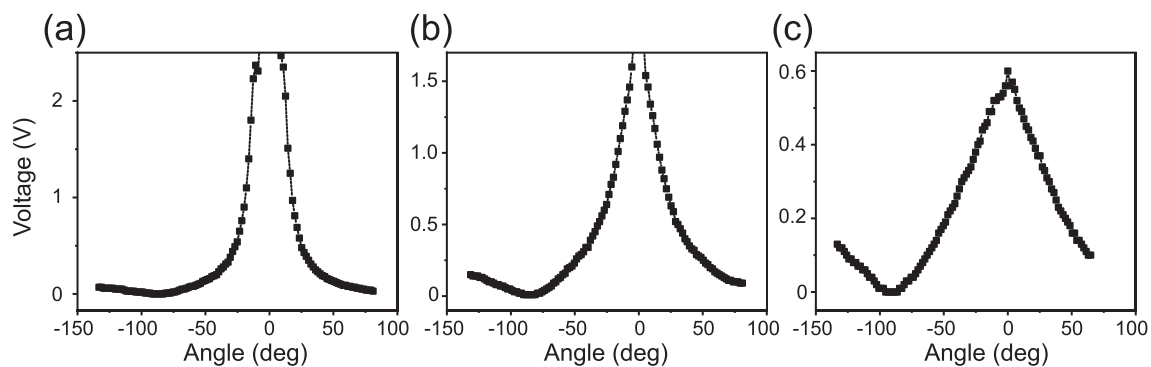


FIG. 5. Angular distribution of the diffusive pattern from the *T. atroviride* bioplate. Voltage photodiode is shown. The distribution broadens as the hyphal density increases from low (a) to medium (b) to high (c). Notably in (c), the transmitted laser spot is not noticeable, indicating a highly efficient diffuser.

work should include achieving a self-standing device; here, the mechanical properties of our fixated mycelium could be enhanced to ease handling. One attractive possibility is to introduce metallic coatings on our film. This approach offers additional possibilities of use for our bioplate, in sensing, optical devices, surface-enhanced Raman scattering, etc. The implementation of natural patterns in the field of optical diffusers or diffraction devices remains a vast area of study.

This work was supported by CONACYT (Mexico) via Grant Nos. IFC-2015-2/1144 and INFR-2018-295138 to B.G.-M. We thank Ana Iris Peña-Maldonado for help with scanning electron microscopy, the Nanoscience and Nanotechnology Research National Laboratory (LINAN) at Instituto Potosino de Investigación Científica y Tecnológica for access to their facilities, and Beatriz Morales Cruzado for help using the spectrometer-integrating sphere.

AUTHOR DECLARATIONS

Conflict of Interest

The authors have no conflicts to disclose.

Author Contributions

Isaac Carrillo-Acuña: Data curation (lead); Investigation (lead); Methodology (equal); Writing – original draft (equal); Writing – review & editing (equal). **Juan Edson Villanueva-Tiburcio:** Investigation (supporting); Methodology (supporting). **Braulio Gutiérrez-Medina:** Conceptualization (lead); Formal analysis (equal); Funding acquisition (lead); Methodology (equal); Project administration (lead); Resources (lead); Supervision (lead); Writing – original draft (equal); Writing – review & editing (equal).

DATA AVAILABILITY

The data that support the findings of this study are available from the corresponding author upon reasonable request.

REFERENCES

- 1 A. Lin and J. Phillips, "Optimization of random diffraction gratings in thin-film solar cells using genetic algorithms," *Sol. Energy Mater. Sol. Cells* **92**, 1689–1696 (2008).
- 2 H. Sai, H. Fujiwara, M. Kondo, and Y. Kanamori, "Enhancement of light trapping in thin-film hydrogenated microcrystalline Si solar cells using back reflectors with self-ordered dimple pattern," *Appl. Phys. Lett.* **93**, 143501–143504 (2008).
- 3 C. Battaglia, C. Hsu, K. Söderström *et al.*, "Light trapping in solar cells: Can periodic beat random?," *ACS Nano* **6**, 2790–2797 (2012).
- 4 H. S. Ko, K. Okamoto, and H. Madarame, "Reconstruction of transient three-dimensional density distributions using digital speckle tomography," *Meas. Sci. Technol.* **12**, 1219–1226 (2001).
- 5 K. D. Kihm, "Applications of laser speckle photography for thermal flow problems," *Opt. Lasers Eng.* **29**, 171–200 (1998).
- 6 J. W. Goodman, *Speckle Phenomena in Optics: Theory and Applications* (Roberts and Company Publishers, Englewood, CO, 2007).
- 7 M. Shokooh-Saremi and R. Magnusson, "Particle swarm optimization and its application to the design of diffraction grating filters," *Opt. Lett.* **32**, 894–896 (2007).
- 8 F. J. Torcal-Milla and L. M. Sanchez-Brea, "Diffraction by random Ronchi gratings," *Appl. Opt.* **55**, 5855–5859 (2016).
- 9 Z. Li, S. W. Chung, J. M. Nam, D. S. Ginger, and C. A. Mirkin, "Living templates for the hierarchical assembly of gold nanoparticles," *Angew. Chem. Int. Ed.* **42**, 2306–2309 (2003).
- 10 K. Govindaraju, S. K. Basha, V. G. Kumar, and G. Singaravelu, "Silver, gold and bimetallic nanoparticles production using single-cell protein (*Spirulina platensis*) Geitler," *J. Mater. Sci.* **43**, 5115–5122 (2008).
- 11 S. V. Kalinin, S. Jesse, W. Liu, and A. A. Balandin, "Evidence for possible flexoelectricity in tobacco mosaic viruses used as nanotemplates," *Appl. Phys. Lett.* **88**, 153902–152007 (2006).
- 12 T. Nomura, S. Tani, M. Ishikawa, H. Tokumoto, and Y. Konishi, "Synthesis of hollow zirconia particles using wet bacterial templates," *Adv. Powder Technol.* **24**, 1013–1016 (2013).
- 13 A. Behjat, H. Nourollahi, and M. A. Bolorizadeh, "Fabrication of organic solar cells with branched cauliflower-like nano structures as a back electrode replicated from a natural template of cicada wing patterns," *Int. J. Opt. Photonics* **11**, 39–48 (2017).
- 14 Q. Yu, K. Sasaki, and T. Hirajima, "Bio-templated synthesis of lithium manganese oxide microtubes and their application in Li⁺ recovery," *J. Hazard. Mater.* **262**, 38–47 (2013).
- 15 R. Selvakumar, N. Seethalakshmi, P. Thavamani, R. Naidu, and M. Megharaj, "Recent advances in the synthesis of inorganic nano/microstructures using microbial biotemplates and their applications," *RSC Adv.* **4**, 52156–52169 (2014).
- 16 G. England, M. Kolle, P. Kim, and J. Aizenberg, "Bioinspired micrograting arrays mimicking the reverse color diffraction elements evolved by the butterfly *Pierella luna*," *Proc. Natl. Acad. Sci. U. S. A.* **111**, 15630–15634 (2014).
- 17 B. Song, V. E. Johansen, O. Sigmund, and J. H. Shin, "Reproducing the hierarchy of disorder for Morpho-inspired, broad-angle color reflection," *Sci. Rep.* **7**, 46023 (2017).
- 18 W. Jo, U. K. Cheang, and M. J. Kim, "Development of flagella bio-templated nanomaterials for electronics," *Nano Converg.* **1**, 10 (2014).
- 19 H. Zhou, J. Xu, X. Liu *et al.*, "Bio-inspired photonic materials: Prototypes and structural effect designs for applications in solar energy manipulation," *Adv. Funct. Mater.* **28**, 1705309–1705327 (2018).
- 20 C. Pouya, D. G. Stavenga, and P. Vukusic, "Discovery of ordered and quasi-ordered photonic crystal structures in the scales of the beetle *Eupholus magnificus*," *Opt. Express* **19**, 11355–11364 (2011).
- 21 Y. Chen, G. Dai, H. Li *et al.*, "Influence of disorders on the optical properties of butterfly wing: Analysis with a finite-difference time-domain method," *Eur. Phys. J. B* **86**, 472 (2013).
- 22 H. Yin, B. Dong, X. Liu *et al.*, "Amorphous diamond-structured photonic crystal in the feather barbs of the scarlet macaw," *Proc. Natl. Acad. Sci. U. S. A.* **109**, 10798–10801 (2012).
- 23 R. P. Jansen, K. Beuck, M. Moch *et al.*, "A closer look at *Aspergillus*: Online monitoring via scattered light enables reproducible phenotyping," *Fungal Biol. Biotechnol.* **6**, 11 (2019).
- 24 G. E. Harman, A. H. Herrera-Estrella, B. A. Horwitz, and M. Lorito, "Trichoderma—From basic biology to biotechnology," *Microbiology* **158**, 1–2 (2012).
- 25 M. Osorio-Concepción, G. R. Cristóbal-Mondragón, B. Gutiérrez-Medina, and S. Casas-Flores, "Histone deacetylase HDA-2 regulates trichoderma atroviride growth, conidiation, blue light perception, and oxidative stress responses," *Appl. Environ. Microbiol.* **83**, e02922 (2017).
- 26 M. Wen, J. Yao, W. K. Wong, and G. C. K. Chen, "Holographic diffuser design using a modified genetic algorithm," *Opt. Eng.* **44**, 085801 (2005).
- 27 J. Goodman, *Introduction to Fourier Optics*, 3rd ed. (Roberts & Co. Publishers, Englewood, CO, 2005).
- 28 K. Lagree, J. V. Desai, J. S. Finkel, and F. Lanni, "Microscopy of fungal biofilms," *Curr. Opin. Microbiol.* **43**, 100 (2018).
- 29 D. Arslan, A. Rahimzadegan, S. Fasold *et al.*, "Toward perfect optical diffusers: Dielectric Huygens' metasurfaces with critical positional disorder," *Adv. Mater.* **34**, 2105868 (2022).
- 30 R. Lampande *et al.*, "Efficient light harvesting in inverted polymer solar cells using polymeric 2D-microstructures," *Sol. Energy Mater. Sol. Cells* **151**, 162–168 (2016).

- ³¹M. D. Fricker, L. L. M. Heaton, N. S. Jones *et al.*, “The mycelium as a network,” *Microbiol. Spectr.* **5**, 1–32 (2017).
- ³²A. E. Posch, O. Spadiut, and C. A. Herwig, “Novel method for fast and statistically verified morphological characterization of filamentous fungi,” *Fungal Genet. Biol.* **49**, 499–510 (2012).
- ³³M. Obert, P. Pfeifer, and M. Sernetz, “Microbial growth patterns described by fractal geometry,” *J. Bacteriol.* **172**, 1180–1185 (1990).
- ³⁴H. Zhou, T. Fan, J. Ding, D. Zhang, and Q. Guo, “Bacteria-directed construction of hollow TiO₂ micro/nanostructures with enhanced photocatalytic hydrogen evolution activity,” *Opt. Express* **20**, A340 (2012).